Generalized Voltage Droop Strategy for Power Synchronization Control in Multi-Terminal DC Grids - an Analytical Approach

Kumars Rouzbehi[1], Weiyi Zhang[1], Jose Ignacio Candela[1], Alvaro Luna[1], and Pedro Rodriguez[1,2]

(1) Technical University of Catalonia
Barcelona, Spain

(2) Abengoa Research
Seville, Spain

Kumars.Rouzbehi@upc.edu

Abstract– **Vector current control based on Phase-locked loop, regardless of its popularity in control of grid-connected converters, performs under the limitation of the short-circuit capacity of the connected ac system.**
A previously proposed method, power-synchronization control (PSC), by L. Zhang et al. has been demonstrated good performance in HVDC links especially in case of weak ac grid interconnection. This method utilizes the internal synchronization mechanism, analogous to the operation of a synchronous machine in ac grids. By using this technique, the voltage source converter (VSC) avoids the instability caused by a standard PLL in a weak ac-system connection. Moreover, a VSC terminal can give the weak ac system strong voltage support, just like a common synchronous machine does.
In this paper, generalized voltage droop (GVD) strategy is developed based on PSC to provide more flexibility in control paradigm of MTDC grids and smoother transition among different operation modes of converter stations. GVD is implemented at the primary layer of a two-layer hierarchical control structure of MTDC grid, and brings about some new features such as fixed power control and fixed dc voltage control, additional to the conventional voltage droop characteristics. The mode transition can be achieved according to the set point given by the secondary layer of the control framework. Analytical justifications are given to demonstrate the effectiveness in each control mode and the capability in soft mode transition.

*Index Terms–***Generalized voltage droop (GVD) control; Multi-terminal DC grids; Power sharing; Power synchronization control.**

I. Introduction

The research conducted in the field of voltage source converter (VSC) based multi-terminal dc (MTDC) grids, including modeling and simulation [1]–[3], short-circuit calculation [4], protection [5]–[6], and control [7]–[9], has experienced an outstanding evolution over the past few years. Such a special attention to MTDC grids is mainly due to two facts: appropriateness of the MTDC grids for the integration of offshore wind farms and possibility of interconnecting several ac networks with even non-identical frequencies. At the present time, there are several ongoing projects worldwide for transmission of bulk offshore wind generations to the ac networks via the MTDC grids [10] – [15]. Several control methods of grid-connected voltage source converters (VSCs) have been proposed. Among them, power-angle control and vector-current control are the two that have been mostly investigated [16]. As mentioned in [16], a severe disadvantage of the former strategy is that the control system does not have the capability to limit the current flowing through the converter due to the absence of current controller or anti wind-up measures. In high-power applications such as MTDC grids, it is highly important to limit the currents to prevent the converter from being blocked (tripped) at disturbances.

The second approach that is very popular is vector-current control[17],[18],[19] that is a current-control-based technology. Thus, it limits the current flowing through the converter during disturbances. However, the potentials of the VSC are not fully utilized with a traditional vector-current control strategy that is commonly aided by a phase-locked loop (PLL) [3], [4]. As discussed in [5], the strength of the ac system relative to the power rating of the HVDC link is described by the short-circuit ratio (SCR). Thus, if the calculated SCR is low, the ac system is considered weak. If the ac system that connects to a MTDC system has a low SCR, the performance of PLL-based vector-current control will be undermined [16]. In contrast, an alternative strategy called PSC is less vulnerable to low SCR. Nevertheless, thus far this control strategy has only been applied in HVDC link [16]. In this paper, power-synchronization control is implemented in MTDC grid. Then, the concept of generalized voltage droop (GVD) control that is proposed in [20], is realized based on PSC to utilize advantages of GVD for having more flexibility in changing of converter stations operation modes. And the controller for power synchronization loop is accordingly designed. GVD

This work was partially supported by Spanish Science Ministry under the project ENE2013-48428-C2-2-R. Any opinions, findings and conclusions or recommendations expressed in this material are those of the authors and do not necessarily reflect those of the host institutions or funders.

is implemented at the primary level of a two-layer hierarchical control structure of MTDC grid, and Performs as an alternative to the conventional voltage droop characteristics of voltage-regulating VSC stations that is controlled based on PSC, providing a higher flexibility and thus controllability to automation of MTDC grids. GVD control strategy can operate in three different operation modes, respectively the conventional voltage droop control, fixed active power control and fixed dc voltage control by setting the GVD characteristics of the VSCs.

The rest of the paper is organized as follows. Implementation of the PSC-based converter control strategy is presented and discussed in Section II. The development of the control scheme employing GVD is introduced in Section III and the control mechanism for each operation mode is illustrated. Conclusions are drawn in Section IV.

II. Control of Multi-Terminal DC Grids

MTDC grids are characterized by the interconnection of several VSC-HVDC stations that are connected together by transmission lines. The main components of the VSC-HVDC terminals include ac circuit breaker, ac transformer, ac filter, phase reactor, voltage source converter and dc capacitor.

For the effective control of the MTDC grid, a two-layer hierarchical control structure, illustrated in Fig. 1, is developed in this paper. In this structure, at the upper level (secondary control), the parameters of the voltage droop controllers of the VSCs are determined, according to the grid conditions and requirements of demand and generation at the ac sides, and sent to the primary control level.

On the other hand, primary control of MTDC grids includes dc voltage regulation at the dc terminals, control of active and reactive power at the point of common coupling (PCC) and maintaining the PCC's ac voltage at the specified set point. As stated before, the most commonly used control strategy for VSC-HVDC stations is based on the vector current control [18]. In this strategy the ac currents and voltages of the converter stations (at the PCC) are transformed into the rotating direct-quadrature (dq) reference frame, synchronized with ac grid voltage by means of a phase-locked loop (PLL).

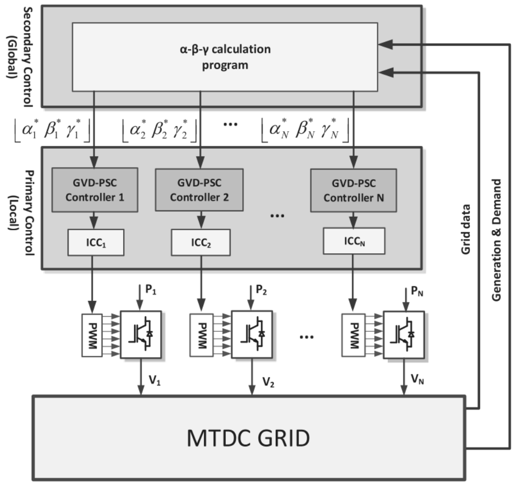

Fig. 1. The proposed hierarchical control framework.

Even though PLL has been largely used for synchronizing VSC with the grid, several investigations have shown that the PLL dynamics might have a negative impact on the performance of VSC-HVDC in case of weak ac system

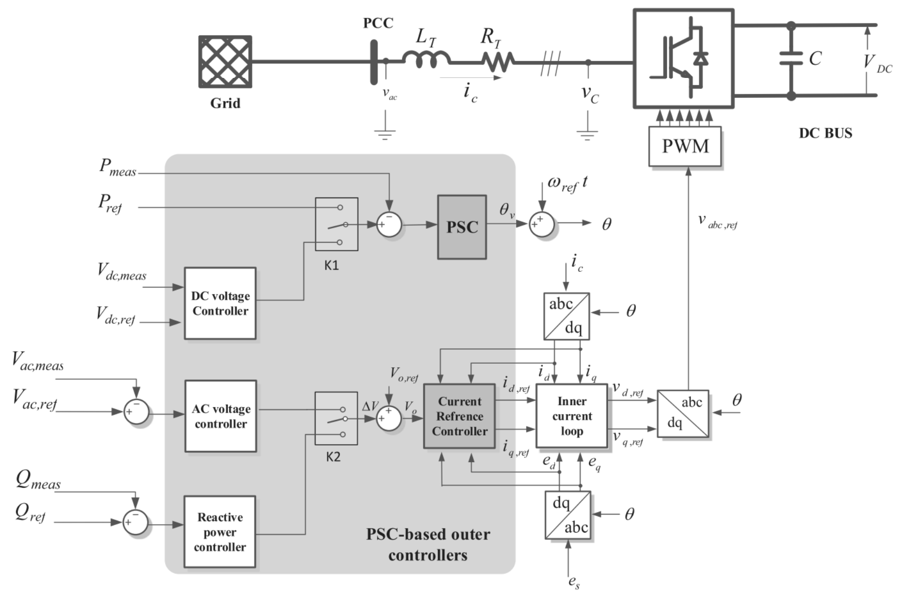

Fig.1. General architecture of the PSC-based control strategy for a VSC-HVDC station.

connections[16]. Oriented to this issue, a series of studies have been carried out employing mechanisms that synchronize the load angle instead of voltage phase, among which PSC arises as a promising strategy as shown in [16]. The general PSC-based control architecture of a VSC-HVDC station is illustrated in Fig. 2. The outer controllers in Fig. 2 are responsible for generating the reference currents for the inner current controller which determines the voltage reference of the converter in the dq frame.

A. Inner Current Controller

The inner current controller (ICC), includes a fast PI controllers which tracks the reference currents, set by the outer controllers, and produces the voltage reference for the converter station. To derive the structure of the ICC, the voltage at PCC (e_s) and ac converter-side voltage (v_c) of Fig. 2 are related by,

$$v_{ac} - v_c = R_T i_c + L_T \frac{di_c}{dt} \tag{1}$$

where, i_c is the current flowing from the ac grid to the converter and R_T and L_T represent the equivalent resistance and inductance installed between the PCC and the converter. Then by applying the dq transformation, (1) can be expressed in dq reference frame by,

$$e_d - v_d = R_T i_d + L_T \frac{di_d}{dt} - \omega L_T i_q \tag{2}$$

$$e_q - v_q = R_T i_q + L_T \frac{di_q}{dt} + \omega L_T i_d \tag{3}$$

where, ω is the angular frequency of the ac grid.

The reference voltages v_d^{ref} and v_q^{ref} produced by ICC are expressed as (4), which are then transformed back into the *abc* reference frame and used to generate the switching signals of the converter.

$$\begin{bmatrix} v_d^{ref} \\ v_q^{ref} \end{bmatrix} = \begin{bmatrix} e_d \\ e_q \end{bmatrix} - \begin{bmatrix} G_{PI}(s) & 0 \\ 0 & G_{PI}(s) \end{bmatrix} \begin{bmatrix} i_d^{ref} - i_d \\ i_q^{ref} - i_q \end{bmatrix} + \omega L_T \begin{bmatrix} i_q \\ -i_d \end{bmatrix} \tag{4}$$

B. PSC-based Outer Controllers

The outer controllers include current reference controller, PSC, dc voltage controller, ac voltage controller and reactive power controller, as shown in Fig. 2.

The current reference controller is responsible for generating the reference signals for the inner current control loops based on the voltage magnitude V_o and the measurement of converter output voltage and current. The calculation of the inner current loop reference is expressed as (5).

$$\boldsymbol{i_{ref}} = \frac{1}{\alpha_c L_T}\left[V_o - \boldsymbol{e_s} - j\omega L_T \boldsymbol{i_c} - H_{HP}(s)\boldsymbol{i_c}\right] + \boldsymbol{i_c} \tag{5}$$

where, α_c is the desired closed-loop bandwidth of the current control, and $H_{HP}(s)$ is a high pass filter structure [16].

The grid synchronization is achieved through PSC by regulating the phase of the output voltage reference, thus regulating the voltage angle difference between the VSC and the ac grid. The controller structure of PSC can vary for different design requirements, and as a simple form, the integral controller with a damping term as (6) is proposed for fast grid synchronization.

$$G_{PSC} = \frac{K_I}{\tau s + 1} \tag{6}$$

Considering mainly inductive impedance at the filter and the transmission line and small signal of the load angle, the active power going through the VSC can be expressed as (7).

$$\Delta P_{inv} = \frac{VV_o}{X}\Delta\theta \tag{7}$$

In (7), V_o and V are respectively the RMS value of the line-to-line converter output voltage and grid voltage, and X the converter output reactance seen from PCC.

Combining (6) and (7), the closed-loop active power regulating transfer function is shown in (8).

$$\frac{P_{inv}}{P_{ref}}(s) = \frac{1}{\mathrm{T}s + D} \tag{8a}$$

$$\mathrm{T} = \frac{\tau X}{K_I V V_o} \tag{8b}$$

$$D = 1 + \frac{X}{K_I V V_o} \tag{8c}$$

According to (8), the settling time of the power synchronization loop t_{ss} is explicitly linked to the control parameter K_I, and the relation is shown in (9) considering 1% as steady state band.

$$t_{ss} \approx 5\mathrm{T} \tag{9}$$

In this way, the active power can be controlled by switching K1 up as shown in Fig. 2. And optionally, the dc link voltage can be directly controlled by switching K1 down with the aid of an additional controller, which can be designed as (10), for instance.

$$P_{ref} = (K_{pd} + \frac{K_{id}}{s})\frac{v_{dc,ref}^2 - v_{dc}^2}{2} \tag{10}$$

Likewise, by selecting the state for the switch K2, either the reactive power or ac voltage is able to be controlled. The ac voltage controller and reactive power controller are respectively designed as shown in (11) and (12).

$$\Delta V = \frac{k\omega_c}{s + \omega_c}(V_{ac,meas} - V_{ac,ref}) \tag{11}$$

$$\Delta V = (K_{PQ} + \frac{K_{IQ}}{s})(Q_{ref} - Q_{meas}) \tag{12}$$

C. Voltage Droop Control

The voltage level at different terminals of an MTDC grid directly influences the flow of dc power between the terminals of the MTDC grid. It is worth noting that unlike ac transmission systems were fixed and identical voltage amplitudes (normally around 1 p.u) are preferred throughout the network, the MTDC grids cannot have the same voltage level over the entire grid, as the power flow between the dc terminals rely on this variable.

The voltage droop control allows regulating the dc voltage within the grid by adjusting the converters currents in such a way that the power balance is guaranteed throughout the grid [19]. In this method a proportional controller is employed, following thus a characteristic, describing a unique relation between the dc voltage and the converter transmitted current/power [20]. The idea behind the voltage-droop control has been inspired by the power-frequency droop control in ac networks, where increase/decrease in demand level leads to frequency drop/rise. Similarly, in an MTDC grid a rise in the dc voltage implies a power surplus in the system, and the dc voltage regulating stations should start to operate in order to re-establish power balance, while dc voltage drop indicates lack of power in the system and the dc voltage regulating stations should start to increase rectification. This is the basics of the voltage droop control for MTDC grids.

A typical voltage droop characteristic shown in Fig. 3 illustrates the idea clearly.

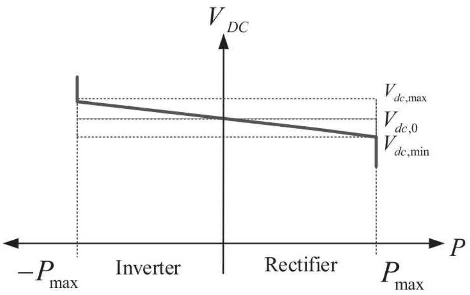

Fig. 3. A conventional (fixed) voltage droop characteristics.

Besides, the implementation of voltage droop characteristics in PSC-based outer controllers is illustrated in Fig. 4.

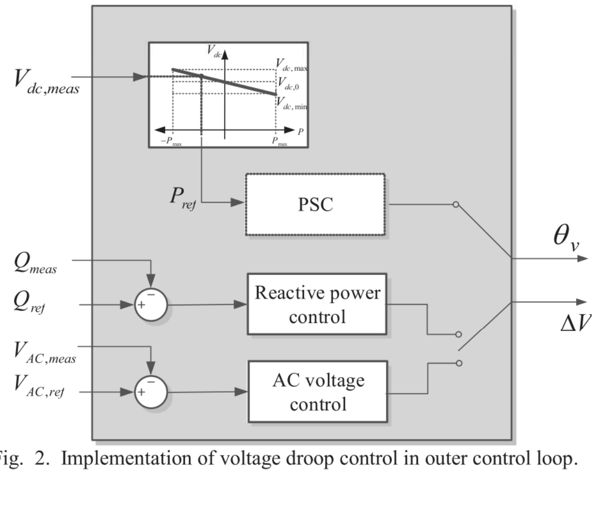

Fig. 2. Implementation of voltage droop control in outer control loop.

Despite of the aforementioned advantages, the voltage droop control shown in Fig. 4 has some drawbacks.

- It is not able to perform full power flow control, as the droop control cannot fix the active power at a constant level.
- It cannot fix the voltage of the dc terminals, if required.

Hence, modifications can be introduced into the voltage droop control to overcome these shortcomings.

III. Generalized Voltage Droop Control

The GVD control is proposed as a generalized design integrating droop control, dc voltage control and PSC. It is able to perform fixed power control, fixed dc voltage control or share power among voltage-regulating converters based on the slopes of voltage droop characteristics, hence shows more flexibility than the conventional voltage droop scheme that is only capable of power-voltage droop control.

It involves three operating modes as shown in Fig. 5, where each mode can be activated by adjusting the coefficient of the generalized voltage droop characteristic, thus offers the possibility of smooth switching among each mode. In this way, the role of a specific VSC is not necessarily fixed during the operation and can smoothly change along with the needs of the system, and the reliability of the system is enhanced as well as the flexibility in secondary control.

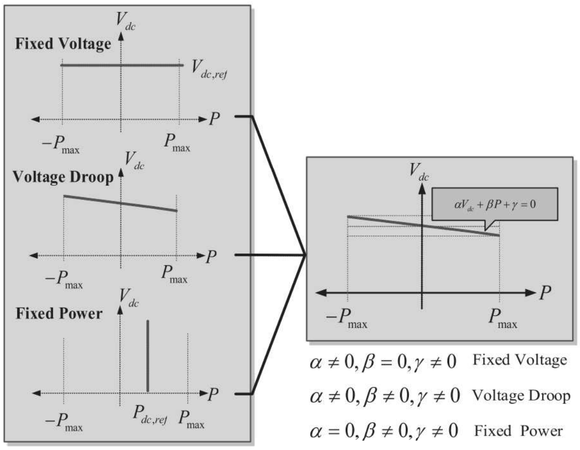

Fig. 5. GVD characteristics with three operation modes.

The GVD characteristic is mathematically expressed by,

$$\alpha V_{dc,meas} + \beta P_{meas} + \gamma = 0 \qquad (13)$$

where, $V_{dc,meas}$ and P_{meas} are the measured voltage and power at dc-side of the VSC station, respectively and α, β and γ are the coefficients of the GVD characteristics.

A. Operating Modes of the GVD Control

The operating modes of the GVD control are explained as follows.

1) Mode 1: Conventional Voltage Droop Control: This mode is employed by choosing $\alpha \neq 0$, $\beta \neq 0$ and $\gamma \neq 0$. In this mode, the conventional voltage droop control is carried out;i.e., when converter's dc voltage starts rising it increases power inversion. On the other hand, if the dc voltage drops the converter injects more power into the dc grid.

For this operating mode, the GVD coefficients are computed based on the dc voltage ($V_{dc,0}$) and power (P_0) associated with an operating point of the corresponding converter. In other words, the following condition must be satisfied,

$$\alpha V_{dc,0} + \beta P_0 + \gamma = 0 \tag{14}$$

In (14) there are three unknown parameters (α, β and γ). Hence, two more equations must be added to solve for α, β and γ. In this paper, the slope of GVD characteristics, m, are assumed constant and pre-defined.

$$m = \frac{\beta}{\alpha} \tag{15}$$

Without any loss of generality, by assuming $\alpha = 1$, one can compute,

$$\beta = m \tag{16}$$

Based on (14) and (16), the γ can be determined as,

$$\gamma = -V_{dc,0} - mP_0 \tag{17}$$

2) Mode 2: Fixed Power Control: In the second mode of operation, the controller fixes the active power of the station to the specified set-point, P_{ref}, by choosing $\alpha = 0$, $\beta \neq 0$ and $\gamma \neq 0$. In this way, the proposed controller will be equivalent to the scheme shown in 2 when K1 is switched up. This mode of operation allows the fixed power control particularly in circumstances a station needs to receive or transfer a particular amount of active power while the remaining power is shared among other stations according to their droop characteristics.

In this mode $\alpha = 0$. Hence, based on (14) and keeping $\beta = m$, which is obtained from the conventional voltage-droop mode,

$$\alpha = 0 \tag{18}$$

$$\beta = m \tag{19}$$

And by setting $P_0 = P_{ref}$, γ can be determined as:

$$\gamma = -\beta P_{ref}\,. \tag{20}$$

According to (20), by adjusting the coefficients β and γ also setting α to zero, the required reference power is obtained.

3) Mode 3: Fixed DC Voltage Control: The third operating mode controls the dc voltage of the station at the specified set-point, $V_{dc,ref}$, with $\alpha \neq 0$, $\beta = 0$ and $\gamma \neq 0$. This mode of operation is useful when it is required to fix the dc voltage of the station at a particular level. Then the task of the dc voltage control and the active power balance within the MTDC grid is assigned to the converter station operating in this mode of the GVD control (like the slack bus in ac grid).

However, this mode cannot be activated by directly setting $\beta = 0$. In this paper a novel strategy is proposed to eliminate the undesirable effect while the switch K1 in Fig. 2 is acting. In this strategy, for constant dc voltage control, the GVD is still operating in the conventional voltage droop mode (i.e. mode 1), but an extremely small value is assigned to coefficient β, which indicates the slope of the GVD characteristics. Hence, the GVD characteristic is almost aligned to the horizontal axis, resembling the fixed voltage control mode. Therefore, under this circumstance the following reference power signal is generated by the GVD characteristic,

$$P_{ref} = \frac{\alpha V_{dc,meas} + \gamma}{-\beta} \tag{21}$$

where, $\beta \approx 0$, and according to (17) γ can be written as:

$$\gamma = -V_{dc,0} - \beta P_0 \tag{22}$$

Now, assuming that $\alpha = 1$, setting $V_{dc,0} = V_{dc,ref}$, and substituting (22) into (21), the following error signal which is sent to the active channel PI controller,

$$e = P_{ref} - P_{meas} = \frac{-1}{\beta}\left(V_{meas} - V_{dc,ref}\right) + P_0 - P_{meas} \tag{23}$$

Since voltage and power signals are in per-unit basis (i.e., are in similar range), and the coefficient $1/\beta$ tends to the infinity, the power error term, $P_0 - P_{meas}$, in (23) can be disregarded compared to the voltage error term $V_{meas} - V_{dc,ref}$. Hence, (23) can be approximated by,

$$e \approx \frac{1}{\beta}\left(V_{dc,ref} - V_{meas}\right) \tag{24}$$

indicating a fixed dc voltage control action of the GVD control. Then the dc voltage regulating loop is modeled as Fig. 6.

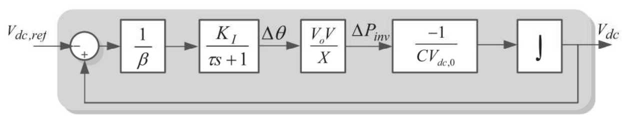

Fig. 6. DC voltage regulating loop when Mode 3 is activated.

According to Fig. 6, dc voltage regulating transfer function is summarized as (25a), which is expressed as a second order parametric transfer function. The natural frequency and damping coefficient are expressed in (25b) and (25c) respectively.

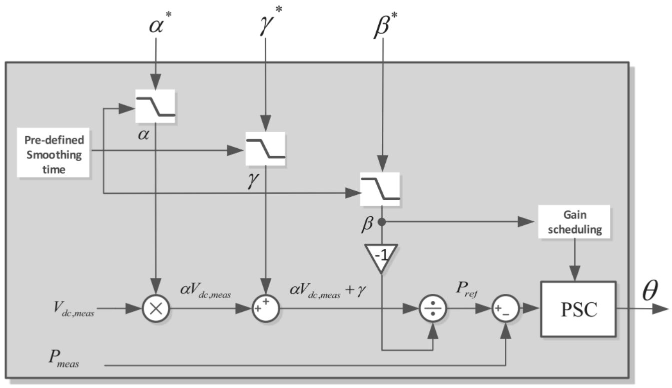

Fig. 7. Implementation of the proposed GVD control with the smooth change in the operating mode

$$\frac{V_{dc}}{V_{dc,ref}}(s)=\frac{\omega_n^{\;2}}{s^2+Ds+\omega_n^{\;2}} \quad (25a)$$

$$D=\frac{1}{\tau} \quad (25b)$$

$$\omega_n=\sqrt{K_I V V_o / \beta \tau X C V_{dc,0}} \quad (25c)$$

where C is the dc link capacitance.

It must be noted that the large value of the gain $1/\beta$ in the error signal of (24) may lead to the instability of the control system. To avoid such adverse effect, a gain scheduling block, as illustrated in Fig. 7., decrease the gain of PSC smoothly, as β tends to zero.

Therefore, it can be remarked that the proposed GVD strategy has much more flexibility than the conventional voltage droop scheme which is only capable of power-sharing based on the droop characteristics of the VSCs.

B. Smooth Change in GVD Operation Modes

In order to allow a smooth change of the GVD characteristic from one mode to another, a smoothing function is employed. In fact, when the GVD is going to change its operating mode, this is carried out by changing its coefficients, α , β and γ , are varied from the old values to the new values, smoothly during the smoothing period of $T_{smoothing}$. This strategy, illustrated in Fig. 7, improves the transient response of the control system during mode change in the GVD characteristics, compared to the abrupt change in the GVD coefficients.

Moreover, such a smooth change policy is applied to the coefficients of the PSC by gain scheduling of K_I as showed in Fig. 7, during transition to the fixed dc voltage control mode.

IV. Conclusion

This paper proposed the application of GVD strategy for PSC-controlled VSC stations in MTDC power grid. The performance of the PSC enhanced by GVD is analyzed and demonstrated to be promising to tackle the shortcoming of PLL-based vector current control in case of weak ac grids, and to improve the flexibility in MTDC grid control.

V. References

[1] L. Jiao, G. Joos, C. Abbey, Z. Fengquan, and B.T. Ooi, "Multi-terminal DC system for wind farms powered by doubly-fed induction generators (DFIGs)," in *proc. PESC 04*, 2004, pp. 1413–1418.

[2] N.R. Chaudhuri, R. Majumder, B. Chaudhuri, J. Pan, and R. Nuqui, "Modeling and stability analysis of MTDC grids for offshore wind farms: A case study on the North Sea benchmark system," in *Proc. 2011 IEEE PES GM*, San Diego, USA, pp. 1–7.

[3] L. Livermore, J. Liang, and J. Ekanayake,"MTDC VSC technology and its applications for wind power," in *Proc. 45 th Int. UPEC*, Cardiff, UK, 2010, pp.1–6.

[4] J. Yang, J.E. Fletcher, and J. O'Reilly, "Short-circuit and ground fault analyses and location in VSC-Based DC network cables," *IEEE Trans. Ind. Electron.*, vol. 59, no. 10, pp. 3827–3837, Oct. 2012.

[5] L. Tang and B.T. Ooi, "Locating and isolating DC faults in multi-terminal DC systems," *IEEE Trans. . Power Del.,* vol. 22, no. 3, pp. 1877–1884, Jul. 2007.

[6] J. Yang, J.E. Fletcher, J. O'Reilly, G.P. Adam, and S. Fan, "Protection scheme design for meshed VSC-HVDC transmission systems of large-scale wind farms," in *Proc. 9th IET International ACDC, 2010*, pp. 1–5.

[7] J. Liang, O.G. Bellmunt, J. Ekanayake, and N. Jenkins, "Control of multi-terminal VSC-HVDC transmission for offshore wind power," in *Proc. EPE* , 2009, pp. 1–10.

[8] J. Beerten, D.V. Hertem, and R. Belmans, "VSC MTDC systems with a distributed DC voltage control - A power flow approach," in *Proc. 2011 IEEE Trondheim PowerTech*, pp. 1-6.

[9] M. Han, L. Xiong, and L. Wan, "Power-synchronization loop for vector current control of VSC-HVDC connected to weak system," in *Proc. 2012 POWERCON*, pp. 1–5.

[10] L. Xu, B.W. Williams, and L. Yao, Liangzhong "Multi-terminal DC transmission systems for connecting large offshore wind farms," *2008 IEEE PES GM.*

[11] X. Chen. W. Lin, H. Sun, J. Wen, N. Li, and L. Yao, "LCC based MTDC for grid integration of large onshore wind farms in Northwest China," in *Proc. 2011 IEEE PESGM*, pp. 1–10.

[12] Y. Fu, Y. Wang, Y. Luo, H. Li, and X. Zhang, "Interconnection of wind farms with grid using a MTDC network," in *Proc. IECON*, 2012, pp. 1031–1036.

[13] X. Chen, H. Sun, J. Wen, W.-J. Lee, X. Yuan, N. Li, and L. Yao, "Integrating Wind Farm to the Grid Using Hybrid Multiterminal HVDC Technology," *IEEE Trans. Ind. Appl.*, vol. 47, no. 2, pp. 965–972, Mar. /Apr. 2011.

[14] J. Blau, "Europe plans a north sea grid," *IEEE Spectrum*, vol. 47, no. 3, pp. 12–13, 2010.

[15] L. Xu and L. Yao, "DC voltage control and power dispatch of a multiterminal HVDC system for integrating large offshore wind farms, " *IET Renewable Power Generation*, vol. 5, no. 3, pp. 223–233, 2011.

[16] L. Zhang, L. Harnefors, and H.-P. Nee, "Power-synchronization control of grid-connected voltage-source converters," *IEEE Trans. Power Syst.,* vol. 25, no. 2, pp. 809–820, 2010.

[17] K. Rouzbehi, A. Miranian, A. Luna, and P. Rodriquez, "Optimized control of multi-terminal DC grids using particle swarm optimization," in *Proc. EPE*, Lille, France, 3–5 Sep 2013, pp. 1–9.

[18] K. Rouzbehi, A. Miranian, A. Luna, and P. Rodriquez, "A novel approach for voltage control of multi-terminal DC grids with offshore wind farms," in *Proc. 2013 IEEE ECCE Asia*, Melbourne, Australia, pp. 965–970.

[19] K. Rouzbehi, A. Miranian, A. Luna, and P. Rodriquez, "A generalized voltage droop strategy for control of multi-terminal DC grids," in *Proc. ECCE, Denver*, USA, 15–19 Sep. 2013, pp. 59–64.

[20] K. Rouzbehi, A. Miranian , J. Candela, A. Luna, and P. Rodriguez, "A generalized voltage droop strategy for control of multi-terminal dc grids," *IEEE Trans. Ind. Appl*., vol.51, no.1, pp.607–618, Jan./Feb. 2015.